Outage Performance of FSO Links with Chirped Gaussian Pulses and Truncated Modeled Time Jitter

D. Kriempardis, P.J. Gripeos, E. Kapotis, H.E. Nistazakis
Section of Electronic Physics and Systems, Department of Physics, National and Kapodistrian University of Athens, Athens, 15784, Greece
dimitriskrie@gmail.com; {pgrypaios; ekapotis;enistaz}@phys.uoa.gr

A.D. Tsigopoulos
Sector of Battle Systems, Naval Operations, Sea Studies, Navigation, Electronics and Telecommunications Hellenic Naval Academy, Piraeus, 18539, Greece
atsigo@snd.edu.gr

Ch. K. Volos
Laboratory of Nonlinear Systems, Circuits & Complexity, Physics Department, Aristotle University of Thessaloniki, Thessaloniki, Greece;
volos@physics.auth.gr

***Abstract* — FSO communications constantly flourish, because of the numerous efficient and economic benefits, highlighted by many researchers and exploited by many manufacturers; however, FSO channels are not free of various performance limitations. This work concerns FSO links' availability estimation by taking into account both, the propagation into a dispersive media and the time jitter influence. Particularly, the truncated normal distribution has been used in order to investigate the time jitter effect on chirped longitudinal Gaussian pulses. The links' performance is presented in terms of either probability of fade or outage probability, in closed form mathematical expressions. The work is concluded with the corresponding numerical results and inferences, using typical and realistic parameters of operating FSO systems.**

Keywords — Optical wireless communications; Group velocity dispersion; Time jitter; Truncated normal distribution; Probability of fade; Outage probability

I. INTRODUCTION

Free space optical (FSO) communications links are cheaply installed and operate without purchasing a license, supporting very high data rate communications, securely [1]–[14]. However, FSO channels are not free of various limitations on the availability and the overall performance of the systems, depending on both the channel's current atmospheric conditions and the link's specifications, such as the bit rate and the link length. Since, contemporary communications require very high data rates hence shorter pulses and longer links, implying long-lasting propagations accompanied by many, accumulated, acting physical phenomena which should be taken into account. For this reason, we investigate the FSO pulse propagation under the action of the group velocity dispersion (GVD) and the time jitter (TJ) effects.

Due to the dispersive media, the GVD is responsible for changes in the shape of the longitudinal pulses during propagation through the atmospheric path, [15], [16], and its influence is stronger as the link length is getting longer and the data rate higher. This is because the broadened pulses may exceed their dedicated time slots, interfering with adjacent slots, i.e. inter-symbol interference - ISI. On the other hand, TJ affects the synchronization between transmitters and receivers, as the detection is not performed at the peak of the pulse, due to the beam scattering, the multipath, the detection delays and any other reason that could trigger a desynchronization between transmitter and receiver. Strong TJ effects may cause severe misdetections, even involving adjacent time slots, inducing bit flips along the bit stream [17]–[20]. Obviously, the shorter the time slot, i.e. faster bit rate, the stronger the influence of TJ effect. Bit misdetections due to strong TJ effect have thoroughly been studied in [21]. In this work, we study the joint influence of GVD and TJ effects, for weak to moderate time jitter which causes misedetections within a range of one time slot, in order to estimate the average irradiance and the outage performance of the system. Another effect which has been studied thoroughly [1]-[14] and affects significantly the system's performance is the scintillation. Its influence could be studied jointly with the above mentioned effects but it is beyond the scope of this work.

The remainder of this work is arranged in the following order: section II hosts the main aspects of the channel model, including the GVD and TJ estimation analysis, in section III the system's expected irradiance is estimated along with the Probability of Fade (PoF) and the Outage Probability (OP), while section IV illustrates the corresponding numerical results, using typical parameters of operating FSO systems, ending up with some interesting conclusions in Section V.

II. CHANNEL MODEL

The optical pulse, of the FSO link under consideration, propagates through the dispersive and turbulent atmosphere with additive white Gaussian noise (AWGN), $\tilde{n}$, zero mean value and variance, $\sigma_N^2 = N_0/2$. The channel is considered as memoryless, ergodic and stationary, with independent and identically distributed (i.i.d.) intensity fading statistics, so that the received, electrical signal, y, is formulated as:

$$y = xs + \tilde{n} \tag{1}$$

where x represents the modulated binary signal, i.e. "0" or "1" bit, and $s=\eta I$ denotes the instantaneous beam intensity, with η and I being the effective photo-current conversion ratio of the receiver and the normalized irradiance of the signal, [22].

A. GVD effect estimation

In general, the refractive index of any medium depends on the wavelength of the propagating signal, affecting the speed of each spectral component, resulting in a pulse spread. In order to evaluate this effect, the refractive index, $n(\lambda)$, should be estimated as a function of the link characteristics, [15], [23], [24]:

$$n(\lambda) = 1 + \frac{77.6 P_h}{T_h}\left[1 + 7.52\cdot 10^{-3}\lambda^{-2}\right]10^{-6} \tag{2}$$

where λ is the operating wavelength in μm, P_h is the atmospheric pressure $P_h = 2.23\cdot 10^{-6}\left(44.41 - 10^{-3}h\right)^{5.256}$ in mbars, T_h is the atmospheric temperature in K and has the form $T_h = 288.19 - 6.49\cdot 10^{-3}h$, as a function of the altitude, h in meters. Thus, the GVD parameter is given as, [15], [16]:

$$\beta_2\left[\frac{ps^2}{km}\right] = \frac{3.5n(\omega)P_h}{2\pi c^2\lambda T_h}10^{15} \quad (3)$$

assuming that $\omega = (2\pi\upsilon/\lambda)10^6$ in rad/s, with υ being the speed of light in the medium in m/s.

Furthermore, by assuming longitudinal chirped Gaussian pulse's envelope, its normalized amplitude after distance z is, [16], [25]:

$$U(z,T) = \frac{T_0}{\sqrt{T_0^2 - i(1+iC)\beta_2 z}}\exp\left\{-\frac{(1+iC)T^2}{2\left[T_0^2 - i(1+iC)\beta_2 z\right]}\right\} \quad (4)$$

where T_0 represents the pulse's half-width at the 1/e intensity point, C stands for the chirp effect, T is the retarded time, representing a time frame of the pulse propagating along the pulse with the group velocity with T=0 corresponding to the pulse's center, [26]. Finally, the instantaneous, normalized irradiance at the receiver, $I = \left|U_{z,T}\right|^2$, is then given as:

$$I = B\exp\left(-T^2/A\right) \quad (5)$$

where $A = T_0^2 + 2C\beta_2 z + T_0^{-2}\left(C^2+1\right)\beta_2^2 z^2$ is the squared pulsewidth and $B = \left[1 + 2T_0^{-2}C\beta_2 z + T_0^{-4}\left(C^2+1\right)\beta_2^2 z^2\right]^{-1/2}$ corresponds to the maximum normalized irradiance's amplitude.

Furthermore, in case of negatively chirped pulses, the formula above implies the existence of a critical distance, z_{c1}, where the irradiance is maximized, given by [26]:

$$z_{c1} = \frac{|C|T_0^2}{\beta_2\left(C^2+1\right)} \quad (6)$$

Also, it is worth noting of another critical distance, $z_{c2}=2z_{c1}$, where the decreasing instantaneous irradiance is equal to the initial irradiance, so that $I_{z=0,T=0} = I_{z_{c2},0}$ [26].

B. TJ effect estimation

Assuming that the TJ could be statistically described by the truncated normal distribution, [26], with mean value μ_T and variance σ_T^2, the corresponding probability density function (PDF) is given as:

$$f_T = \frac{\exp\left[-\frac{(T-\mu_T)^2}{2\sigma_T^2}\right]}{\sqrt{2\pi}\sigma_T\left(\Phi_{T_2} - \Phi_{T_1}\right)}, \quad T_1 \le T \le T_2 \quad (7)$$

where $\Phi_{T_i} = 0.5\left\{1 + erf\left[(T_i - \mu_T)/\left(\sqrt{2}\sigma_T\right)\right]\right\}$ for i=1,2.

From (5), the value of T could be obtained as:

$$T = \pm\sqrt{A\ln\left(B/I_j\right)} \quad (8)$$

and using the random variable (RV) transformation, the resulting PDF as a function of I_j is given as:

$$f_{I_j}\left(I_j\right) = \frac{f_T\left[\sqrt{\ln\left(B/I_j\right)}\right]}{\left|dI_j/dT\right|_{T=+\sqrt{A\ln\left(B/I_j\right)}}} + \frac{f_T\left[-\sqrt{\ln\left(B/I_j\right)}\right]}{\left|dI_j/dT\right|_{T=-\sqrt{A\ln\left(B/I_j\right)}}} \quad (9)$$

Finally the PDF of I_j, caused by the GVD and the TJ effect, is obtained by:

$$f_{I_j}\left(I_j\right) = \frac{A\cosh\left(\frac{\sqrt{A\ln\left(B/I_j\right)}\mu_T}{\sigma_T^2}\right)\exp\left(-\frac{A\ln\left(B/I_j\right) + \mu_T^2}{2\sigma_T^2}\right)}{\sigma_T Z\sqrt{A\ln\left(B/I_j\right)}} \quad (10)$$

where $Z = \Phi_{T_2} - \Phi_{T_1}$. Note that normalized irradiance, I_j, ranges between the maximum value B and the minimum value $I_{j,0} = B\exp\left[-T_{sl}^2/(4A)\right]$, corresponding to the normalized irradiance at both edges of the time slot, $T = \pm T_{sl}/2$.

III. Link Performance

The receiver's instantaneous electrical signal-to-noise ratio (SNR), $\gamma_j = \left(\eta I_j\right)^2/N_0$, is perpetually fluctuating, owing to the beam's propagation through the atmosphere. The average electrical SNR, is given as $\bar{\gamma}_j = \left(\eta E\left[I_j\right]\right)^2/N_0$, with $E[I_j]$ being the expecting value of I_j, [27], [28]. For simplicity, in the following analysis it is assumed that, $\mu_T = 0$, i.e. symmetrical distributed normalized irradiance around pulse's center.

A. Expected Irradiance estimation

The expected value of I_j, is estimated as [29]:

$$E\left[I_j\right] = \int_{I_{j,0}}^{B} I_j f_{I_j}\left(I_j\right)dI_j \quad (11)$$

Next, using Eq. (10) and a variable transformation $y = \sqrt{A\ln\left(B/I_j\right)}$, the above integral gives:

$$E\left[I_j\right] = \frac{\sqrt{2\pi A}B^2}{Z\Theta}\left\{erf\left[\frac{\Theta T_{sl}/2}{\sqrt{2A}\sigma_T}\right]\right\} \quad (12)$$

where $\Theta = \sqrt{4\sigma_T^2 + A}$.

B. Probability of fade estimation

The PoF corresponds to the probability of a critical drop-off below a sensitivity threshold in terms of receiving irradiance, $I_{j,th}$, and is given as, [26]:

$$P_{fade} \equiv F_{I_j}\left(I_{j,th}\right) = \int_0^{I_{j,th}} f_{I_j}\left(I_j\right)dI_j \quad (13)$$

where $F_{I_j}\left(I_{j,th}\right)$ stands for the corresponding cumulative density function (CDF). The integral of (13) concludes to:

$$P_{fade}(I_{th}) = \frac{\sqrt{2\pi A}B}{Z\Lambda}\left\{erf\left[\frac{\Lambda T_{sl}/2}{\sqrt{2A}\sigma_T}\right] - erf\left[\frac{\sqrt{\ln\left(B/I_{j,th}\right)}}{\sqrt{2}\Lambda^{-1}\sigma_T}\right]\right\} \quad (14)$$

where $\Lambda = \sqrt{2\sigma_T^2 + A}$.

C. Outage probability estimation

OP shows the critical drop-off below a specific threshold in terms of receiving instantaneous SNR and is given as, [28]:

$$F_{\gamma_j}\left(\gamma_{j,th}\right) = \int_{\gamma_{j,0}}^{\gamma_{j,th}} f_{\gamma_j}\left(\gamma_j\right) d\gamma_j \qquad (15)$$

where $\gamma_j = \frac{I_j^2 \bar{\gamma}}{\left(E\left[I_j\right]\right)^2}$ and $\gamma_{j,0} = \frac{B^2 \bar{\gamma}_j}{\left(E\left[I_j\right]\right)^2} \exp\left(-\frac{T_{sl}^2}{4A}\right)$. From (15), the OP performance gives:

$$P_{out} = \frac{\sqrt{2\pi}AB}{ZE\left[I_j\right]\Lambda}\left\{ erf\left[\frac{\Lambda T_{sl}}{\sqrt{8A}\sigma_T}\right] - erf\left[\frac{\sqrt{\ln\left(\frac{\bar{\gamma}_j \gamma_{j,th}^{-1} B^2}{E^2\left[I_j\right]}\right)}}{\sqrt{4\Lambda^{-1}}\sigma_T}\right]\right\} \qquad (16)$$

IV. Numerical Results

In this section the availability of an FSO system with longitudinal Gaussian pulses is estimated through Eqs (14) and (16), taking into account both the TJ and the GVD effects, and the corresponding outcomes are presented. Supposing a typical wireless optical link of 10Gbps, operating at 1.55μm, 30m above the earth surface, with σ_T=7ps, pulsewidth T_0 equal to either 3 or 5 ps and chirp parameter, C=20 or -20.

Figure 1 illustrates the PoF of a chirped pulse versus the value of the normalized irradiance threshold, probed at both critical distances, z_{c1} and $z_{c2}=2z_{c1}$, for each case. It should be mentioned here that the values of z_{c1} and z_{c2} depend on the pulsewidth. In general, the PoF declines as the normalized irradiance threshold gets lower, in any studied case. Focusing on cases with opposite chirp parameter, it turns out that the corresponding curves are intersected in I_{th} values which are higher for the cases at $z=z_{c2}$ comparing with those at $z=z_{c1}$.

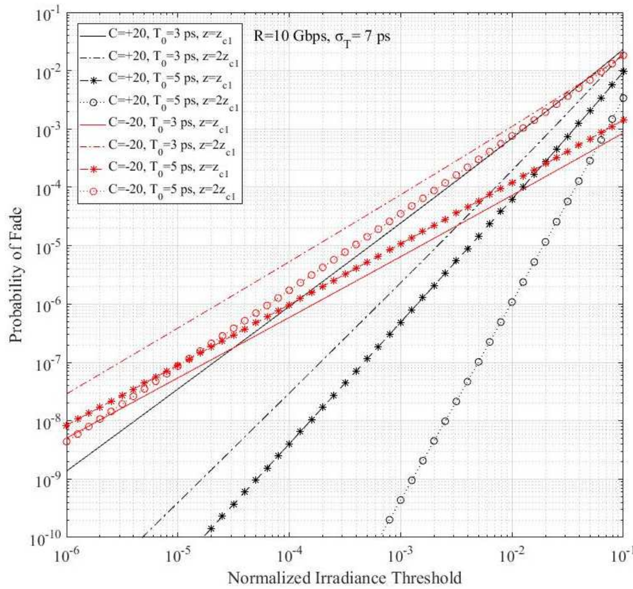

Fig. 1. Probability of fade as a function of the normalized irradiance threshold, for standard bit rate and TJ effect, with various T_0 values and opposite chirp parameter, C, probed at both critical distances, z_{c1} and z_{c2}.

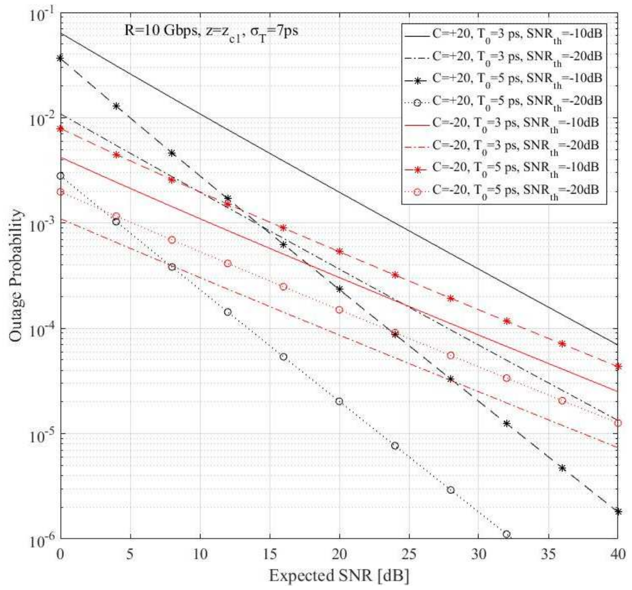

Fig. 2. Outage probability as a function of the expected SNR, probed at critical distance z_{c1}, for standard bit rate and TJ effect, with various T_0 parameter, SNR thresholds and opposite chirp parameters.

In Figure 2, the OP is estimated as a function of the expected SNR for $z=z_{c1}$ and two SNR thresholds, i.e. -10 dB and -20 dB. In all cases, OP decreases as the expected SNR increases, while all cases with SNR threshold -20 dB are less probable to be appeared, compared to those of -10 dB threshold.

V. Conclusions

In this work, the FSO link outage performance is investigated, assuming longitudinal Gaussian pulses under the action of TJ and GVD effects. The TJ is studied through the truncated normal distribution model and new mathematical expressions are derived for the straightforward estimation of the probability of fade and outage probability. The obtained expressions have been used in order to calculate the outage performance of FSO systems with realistic parameter values and their outcomes are presented. From the expressions and the figures, it can be seen that the chirp effect and the longitudinal pulsewidth affect significantly the system's characteristics and performance.

Acknowledgment

The authors acknowledge funding from National and Kapodistrian University of Athens (NKUA), Special Account for Research Grants (SARG).

References

[1] S. Arnon, *Optical Wireless Communications*. New York: Marcel Dekker Inc., 2003.

[2] D. Kedar and S. Arnon, "Urban optical wireless communication networks: The main challenges and possible solutions," *IEEE Commun. Mag.*, vol. 42, no. 5, 2004, doi: 10.1109/MCOM.2004.1299334.

[3] W. Gappmair, S. Hranilovic, and E. Leitgeb, "Performance of PPM on terrestrial FSO links with turbulence and pointing errors," *IEEE Commun. Lett.*, vol. 14, no. 5, 2010, doi: 10.1109/LCOMM.2010.05.100202.

[4] W. Gappmair and S. S. Muhammad, "Error performance of PPM/Poisson channels in turbulent atmosphere with gamma-gamma distribution," *Electron. Lett.*, vol. 43, no. 16, 2007, doi: 10.1049/el:20070901.

[5] T. A. Tsiftsis, H. G. Sandalidis, G. K. Karagiannidis, and M. Uysal, “Optical wireless links with spatial diversity over strong atmospheric turbulence channels,” *IEEE Trans. Wirel. Commun.*, vol. 8, no. 2, 2009, doi: 10.1109/TWC.2009.071318.

[6] T. Kamalakis, T. Sphicopoulos, S. S. Muhammad, and E. Leitgeb, “Estimation of the power scintillation probability density function in free-space optical links by use of multicanonical Monte Carlo sampling,” *Opt. Lett.*, vol. 31, no. 21, 2006, doi: 10.1364/ol.31.003077.

[7] H. Henniger and O. Wilfert, “An introduction to free-space optical communications,” *Radioengineering*, vol. 19, no. 2, 2010.

[8] G. Z. and P. W., “Terrestrial Free-Space Optical Communications,” in *Mobile and Wireless Communications Network Layer and Circuit Level Design*, 2010.

[9] A. K. Majumdar, “Free-space laser communication performance in the atmospheric channel,” *J. Opt. Fiber Commun. Reports*, vol. 2, no. 4, 2005, doi: 10.1007/s10297-005-0054-0.

[10] H. Kaushal and G. Kaddoum, “Underwater Optical Wireless Communication,” *IEEE Access*, vol. 4, 2016, doi: 10.1109/ACCESS.2016.2552538.

[11] Y.-C. Chi, D.-H. Hsieh, C.-T. Tsai, H.-Y. Chen, H.-C. Kuo, and G.-R. Lin, “450-nm GaN laser diode enables high-speed visible light communication with 9-Gbps QAM-OFDM,” *Opt. Express*, vol. 23, no. 10, 2015, doi: 10.1364/oe.23.013051.

[12] Y. Coello, B. Xu, T. L. Miller, V. V. Lozovoy, and M. Dantus, “Group-velocity dispersion measurements of water, seawater, and ocular components using multiphoton intrapulse interference phase scan,” *Appl. Opt.*, vol. 46, no. 35, 2007, doi: 10.1364/AO.46.008394.

[13] M. P. Ninos, H. E. Nistazakis, and G. S. Tombras, “On the BER performance of FSO links with multiple receivers and spatial jitter over gamma-gamma or exponential turbulence channels,” *Optik (Stuttg).*, vol. 138, 2017, doi: 10.1016/j.ijleo.2017.03.009.

[14] H. G. Sandalidis, T. A. Tsiftsis, G. K. Karagiannidis, and M. Uysal, “BER performance of FSO links over strong atmospheric turbulence channels with pointing errors,” *IEEE Commun. Lett.*, vol. 12, no. 1, 2008, doi: 10.1109/LCOMM.2008.071408.

[15] H. Lu, W. Zhao, and X. Xie, “Analysis of temporal broadening of optical pulses by atmospheric dispersion in laser communication system,” *Opt. Commun.*, vol. 285, no. 13–14, 2012, doi: 10.1016/j.optcom.2012.02.094.

[16] G. Agrawal, *Nonlinear Fiber Optics*. 2006.

[17] G. P. Agrawal, *Fiber-Optic Communication Systems: Fourth Edition*. 2011.

[18] Z. Ghassemlooy, S. Arnon, M. Uysal, Z. Xu, and J. Cheng, “Emerging Optical Wireless Communications-Advances and Challenges,” *IEEE J. Sel. Areas Commun.*, vol. 33, no. 9, 2015, doi: 10.1109/JSAC.2015.2458511.

[19] V. S. Grigoryan, C. R. Menyuk, and R. M. Mu, “Calculation of timing and amplitude jitter in dispersion-managed optical fiber communications using linearization,” *J. Light. Technol.*, vol. 17, no. 8, 1999, doi: 10.1109/50.779156.

[20] A. Mecozzi, C. B. Clausen, M. Shtaif, S. G. Park, and A. H. Gnauck, “Cancellation of timing and amplitude jitter in symmetric links using highly dispersed pulses,” *IEEE Photonics Technol. Lett.*, vol. 13, no. 5, 2001, doi: 10.1109/68.920746.

[21] G. D. Roumelas, H. E. Nistazakis, E. Leitgeb, A. N. Stassinakis, and G. S. Tombras, “On the performance of optical wireless communication links impaired by time jitter, M-turbulence and pointing errors,” *Opt. Commun.*, vol. 472, 2020, doi: 10.1016/j.optcom.2020.126033.

[22] G. D. Roumelas, H. E. Nistazakis, A. N. Stassinakis, G. K. Varotsos, A. D. Tsigopoulos, and G. S. Tombras, “Time Jitter, Turbulence and Chromatic Dispersion in Underwater Optical Wireless Links,” *Technologies*, vol. 8, no. 1, 2019, doi: 10.3390/technologies8010003.

[23] W. O. Popoola, Z. Ghassemlooy, C. G. Lee, and A. C. Boucouvalas, “Scintillation effect on intensity modulated laser communication systems-a laboratory demonstration,” *Opt. Laser Technol.*, vol. 42, no. 4, 2010, doi: 10.1016/j.optlastec.2009.11.011.

[24] L. C. Andrews and R. L. Phillips, *Laser beam propagation through random media: Second edition*. 2005.

[25] D. Marcuse, “Pulse distortion in single-mode fibers 3: Chirped pulses,” *Appl. Opt.*, vol. 20, no. 20, 1981, doi: 10.1364/ao.20.003573.

[26] A. N. Stassinakis, H. E. Nistazakis, K. P. Peppas, and G. S. Tombras, “Improving the availability of terrestrial FSO links over log normal atmospheric turbulence channels using dispersive chirped Gaussian pulses,” *Opt. Laser Technol.*, vol. 54, 2013, doi: 10.1016/j.optlastec.2013.06.008.

[27] X. Zhu and J. M. Kahn, “Free-space optical communication through atmospheric turbulence channels,” *IEEE Trans. Commun.*, vol. 50, no. 8, 2002, doi: 10.1109/TCOMM.2002.800829.

[28] H. G. Sandalidis and T. A. Tsiftsis, “Outage probability and ergodic capacity of free-space optical links over strong turbulence,” *Electron. Lett.*, vol. 44, no. 1, 2008, doi: 10.1049/el:20082495.

[29] G. K. Varotsos, H. E. Nistazakis, and G. S. Tombras, “OFDM RoFSO links with relays over turbulence channels and nonzero boresight pointing errors,” *J. Commun.*, vol. 12, no. 12, 2017, doi: 10.12720/jcm.12.12.644-660.